Interaction Between a Turbulent Air Stream and a Moving Water Surface

THOMAS J. HANRATTY and JAMES M. ENGEN

University of Illinois, Urbana, Illinois

The interaction between a turbulent air stream and a water film flowing parallel to it was studied. The variables explored were the liquid flow rate, the gas flow rate, and the film height. The data were correlated in terms of a liquid and a gas Reynolds number. Thinner films or films having a lower Reynolds number were more stable. For the experiments reported in this research the transition from a smooth surface to a surface possessing two-dimensional waves occurs at $hU_\tau\rho_{liquid}/\mu_{liquid}$ of about 520. Transition from two-dimensional waves to a "pebbled" surface occurs at a value of this parameter of about 600. Theories presented in the literature for the initiation of waves on a liquid surface do not adequately describe the experimental results.

Problems involving the simultaneous flow of a gas stream and a liquid film are commonly met in engineering practice. Film coolers, falling-film-absorption towers, condensers, and the transportation of liquid-vapor mixtures are examples of processes involving such two-phase flow problems. A more thorough understanding of these processes could be derived from a better understanding of the nature of the interaction at the interface of the liquid and gas.

If a gas is blown parallel to a liquid surface, it will exert a drag on the surface and cause the liquid to flow. The drag will increase with gas flow. At high enough flows the surface will become unstable and waves will form. The drag of the gas on the liquid and the velocity profile in the gas then will be dependent upon the structure of the liquid surface. At extremely high flows liquid will be torn from the surface and dispersed in the gas stream.

The experiments described in this paper were undertaken to examine the interaction of an air stream and a water film flowing parallel to it. As they were carried out in a rectangular channel having an aspect ratio of 12:1, the gas flow could be considered as two dimensional. The test section was long enough for the height of the liquid film to have reached an equilibrium condition; there was no change in the momentum flow; and the pressure drop was a function of only the drag at the enclosing surfaces. The channel was made of transparent plastic so that the condition of the interface might be observed. Measurements of the pressure drop and of the velocity profile in the gas reflected the effect of changes of the liquid surface upon the flow in the gas phase.

James M. Engen is at present with Archer-Daniels-Midland Company, Minneapolis, Minnesota.

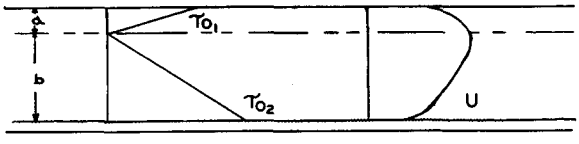

Fig. 1. Shear stress and velocity profile.

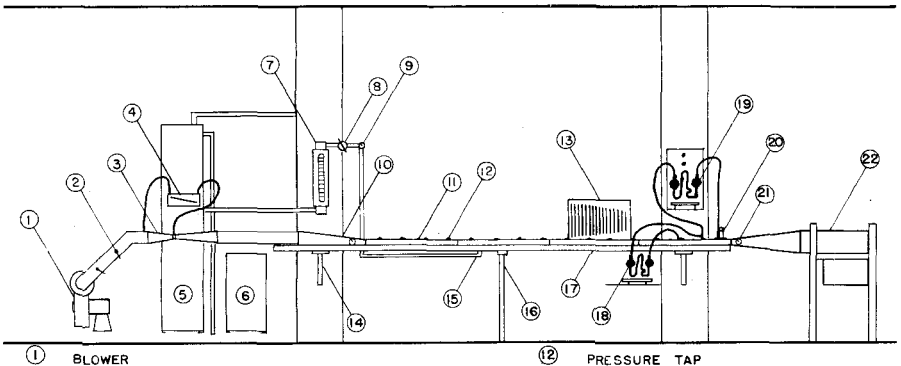

Fig. 2. Sketch of equipment.

THEORY

Flow in the Liquid Film

At low gas velocities where the surface of the liquid film is smooth, the liquid flow would be laminar. The Navier-Stokes equation for a two-dimensional flow may be used to relate the velocity distribution and the volumetric flow in the liquid to the drag of the gas at the surface.

$$u\frac{\partial u}{\partial x} + v\frac{\partial u}{\partial y} = -\frac{1}{\rho}\frac{\partial P}{\partial x} + \frac{\mu}{\rho}\frac{\partial^2 u}{\partial y^2} \qquad (1)$$

For a liquid film with a stable thickness

$$v = 0$$

$$\frac{\partial u}{\partial x} = 0$$

and the pressure drop in the liquid is equal to the pressure drop in the gas. Equation (1) becomes

$$\frac{1}{\rho}\frac{\partial P}{\partial x} = \frac{\mu}{\rho}\frac{\partial^2 u}{\partial y^2} \qquad (2)$$

If the boundary conditions

$$u = 0 \qquad \text{at } y = 0$$

$$g_c\tau_{0_2} = \mu\frac{\partial u}{\partial y} \qquad \text{at } y = h$$

are employed, Equation (2) may be integrated to give

$$u = \frac{g_c}{\mu}\frac{dP}{dx}\frac{y^2}{2} - \frac{g_c}{\mu}\frac{dP}{dx}hy + \frac{g_c}{\mu}\tau_{0_2}y \qquad (3)$$

The volumetric flow rate is

$$Q = \int_0^h u\,dy \qquad (4)$$

$$Q = \frac{g_c}{\mu}\frac{dP}{dx}\frac{h^3}{6} - \frac{g_c}{\mu}\frac{dP}{dx}\frac{h^3}{2} + \frac{g_c}{\mu}\tau_{0_2}\frac{h^2}{2}$$

When the liquid surface is wavy or when the flow is turbulent, no simple expressions such as Equations (3) and (4) can be obtained.

Practically all the theories (*1*) for surface waves have been developed for nonviscous fluids. Although these theories would not be useful in predicting the volumetric flow in the film, they do give a relation between the wave velocity and

TABLE 1

COMPARISON OF ACTUAL AND PREDICTED WAVE LENGTHS

Run No.	t Strob (sec.)	λ^* (cm.)	c^* (cm./sec.)	$t^* = \lambda^*/c^*$ (sec.)	c^{**}calc. (cm.)/(sec.)	Condition
66	0.046	1	30	0.033	25	Two-dimensional waves
67	0.050	1.25	23	0.044	24	Two-dimensional waves
68	0.040	1	30	0.033	25	Two-dimensional waves
69	0.040	0.50	30	0.017	31	Squalls
70	0.054	0.50	20	0.025	31	Squalls

*visual observations.
**using λ^* and Equation (6).

the wave length which approximates the properties of some liquid surfaces observed in this research. For a two-dimensional wave in an irrotational fluid of height h, Lamb (*1*) gives the following expression:

$$c^2 = \frac{g\lambda}{2\pi}\tanh\left(\frac{2\pi h}{\lambda}\right) + \frac{2\pi T}{\rho\lambda}\tanh\left(\frac{2\pi h}{\lambda}\right) \qquad (5)$$

When $h > \frac{1}{2}\lambda$, the equation reduces approximately to

$$c^2 = \frac{g\lambda}{2\pi} + \frac{2\pi T}{\rho\lambda} \qquad (6)$$

The wave length may also be described in terms of the time of oscillation t by using the relation

$$c = \lambda/t \qquad (7)$$

Substituting for c in Equation (6) one obtains

$$\lambda^2 - \frac{g\lambda t^2}{2\pi} - \frac{2\pi T t^2}{\rho\lambda} = 0 \qquad (8)$$

Flow in the Gas

For practically all the experiments reported in this paper the gas was turbulent. Except for the immediate vicinity of the wall a turbulent-flow field in a smooth channel may be described by an empirical equation of the form

$$u^* = A \log y^* + B \qquad (9)$$

For very small-sized roughnesses on the walls Equation (9) is still valid and the surface may be considered "hydraulically smooth." For sufficiently large roughnesses the shear stress at the surface τ_0 will increase as the size of the roughness increases. Likewise, for such a surface the constant B will be dependent upon the surface condition. As the roughness size is increased, a situation is eventually reached at which the flow profile is independent of the fluid viscosity. Such a condition is described as a "completely roughened" surface and the velocity profile data may be correlated in terms of the roughness size k_s.

$$u^* = A \log y/k_s + C \qquad (10)$$

The constant A describing the slope in Equations (9) and (10) would be the same. For a surface which has been completely roughened with sand Schlichting (*2*) gives the following equation:

$$u^* = 5.75\,\frac{y}{k_s} + 8.5 \qquad (11)$$

This equation may be used to calculate an "equivalent sand roughness" for non-smooth liquid surfaces.

In the experiments described in this paper the gas flowed through a channel with an upper surface that may be considered "hydraulically smooth" and a lower surface that consisted of a water film moving slowly relative to the gas flow. If the liquid surface is not smooth the shear stress possibly might be larger at the bottom than at the top of the enclosed gas space. The velocity profile in the gas will be distorted as indicated in Figure 1. The maximum in the velocity profile will be a condition of zero stress. Momentum balances may be written for a unit width of the channel to give expressions which relate the distortion of the velocity profile to the shear stresses at the upper and lower surfaces.

$$a \times 1 \times \Delta P = \tau_{0_1} \times 1 \times \Delta L \qquad (12)$$

$$b \times 1 \times \Delta P = \tau_{0_2} \times 1 \times \Delta L \qquad (13)$$

If the location of the maximum in the velocity profile, the location of the liquid surface, and the pressure drop are known, the shear stress at both surfaces can be calculated.

DESCRIPTION OF THE EXPERIMENTS

A sketch of the experimental equipment is shown in Figure 2. The rectangular channel, which was 1.016 in. high and 12 in. wide, was made of Plexiglas in four sections, each 4 ft. long. The first and second were air-stream calming sections. The second section had slots cut in the sides to hold a flat 20-gauge galvanized iron sheet. This sheet was held 1/16 in. from the bottom by brass spacers; the water entered under it and flowed out forming an even film. The third and fourth sections were calming sections for film entry effects. The fourth served also as a test section.

Pressure taps glued over 1/64-in. holes in the top wall were placed at 1-ft. intervals along the length. Velocity measurements were made with an impact tube at a position 6 in. from the exit of the channel. The impact tube, which was mounted to a traversing mechanism that allowed its position to be measured to 0.001 in., was made from a stainless steel hypodermic needle having a 0.032-in. I.D. and a 0.050-in. O.D. Its leading edge was rounded into a hemispherical shape and it was soldered into a $\frac{1}{8}$-in. brass tube with a 1/16-in. I.D.

The impact pressure and the static pressure drop were measured with a Wahlen micromanometer (*3*) that had a precision of ± 0.0005 in. methanol over a 1-in. range.

The height of the liquid film was measured in two ways; neither was completely satisfactory. The impact tube was brought to the level of the liquid surface and was positioned by being looked at from above and below the film in order to eliminate the illusion of the meniscus rising on the sides of the tube. This method works well for smooth films; however, it is difficult to employ when the surface is rough. A machinist's scale was placed on the outside wall, and with care one could measure the liquid height within 1/64 in. at the first transition and within 2/64 in. at the second transition.

The wave velocity was approximated by timing the travel of a wave over a 3- to 5-ft. length with a stop watch, although a Strobotac was used in some runs. The frequency chosen with the instrument was

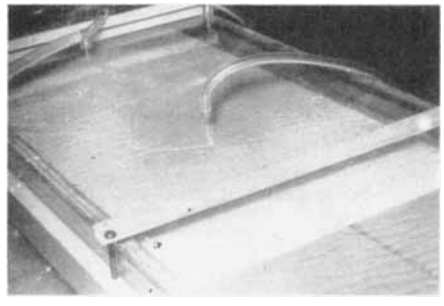

Fig. 3. Photograph of two-dimensional waves

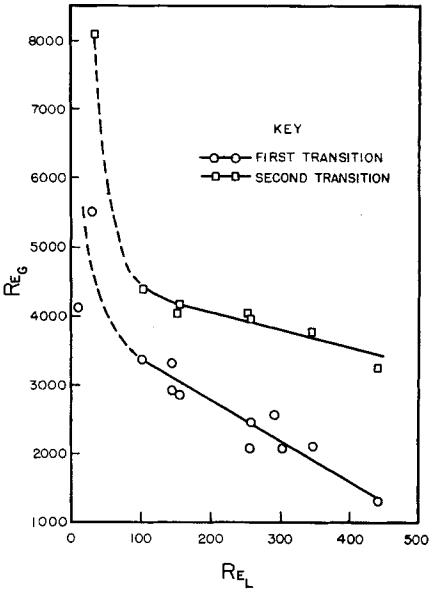

Fig. 4. Re_G vs. Re_L for first two transitions.

that frequency which caused a change in direction of the image.

RESULTS

The effect of water height, liquid flow rate, and gas flow rate was explored under conditions that prevented these quantities from being varied independently. Results were obtained over a range of mean air velocities of 3.8 to 178 ft./sec. and of Re_G based on the thickness of the gas phase H from 945 to 84,000. The liquid height varied from 0.16 to 0.21 in.; the mean liquid velocity ranged from 0.01 to 0.30 ft./sec.; and the Re_L, from 11.9 to 508.

The effect of the gas flow upon the liquid can be described in terms of five types of liquid surfaces: (1) smooth, (2) two-dimensional waves, (3) squalls, (4) roll waves, and (5) dispersed flow.

Two-dimensional Waves

The first disturbance that appeared on the liquid surface as the gas rate was increased was small ripples that quickly formed two-dimensional waves. For an average film thickness greater than $\frac{1}{8}$ in., these two-dimensional waves were nearly 1 cm. apart and traveled at a velocity of from 0.75 to 1 ft./sec. They were low-amplitude waves with heights less than 0.005 in. in all cases. As shown in Figure 3, they were curved; however they extended the complete width of the channel. The relation between the wave velocity and wave length could be approximated by Equation (6). (See Table 1.)

A transition point to a disturbed surface was defined as the point where the first small ripples appeared. Except at very low liquid rates this was coincident with the point at which they disappeared. The gas velocity at which waves first appeared depended on the flow conditions in the liquid. Since the liquid height and liquid flow rate could not be varied independently, the exact role of these two variables in effecting the transition was not ascertained. Results on the effect of liquid flow conditions upon the transition gas velocity are tabulated in Table 2. For Re_L less than 100, U_{max} varied from 3.8 to 9.0 ft./sec. Figure 4 shows the relation between Re_G and Re_L at the first transition. Figure 5 shows the relation between Re_G and the liquid height. A Reynolds number expressed in terms of both the gas and liquid flow properties may be defined at the transition point as

$$Re^* = \frac{hU_\tau \rho_{liquid}}{\mu_{liquid}}$$

Since pressure-drop measurements were made only for runs at the first transition, the parameter τ_0, could be calculated only for a fraction of the data obtained. As shown in Table 3, the transition point occurred at a value of Re^* of approximately 520.

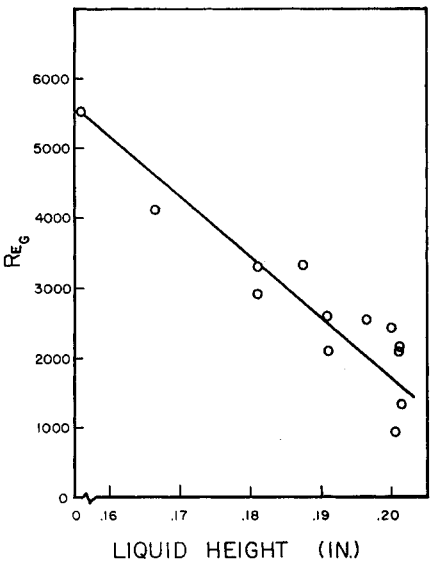

Fig. 5. Re_G vs. liquid height for first transition.

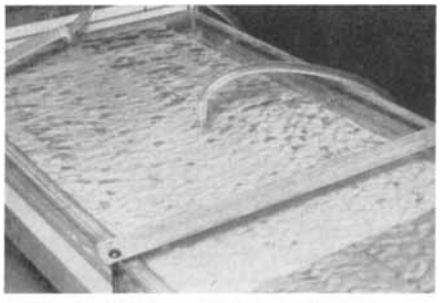

Fig. 6. Photograph of squall surface.

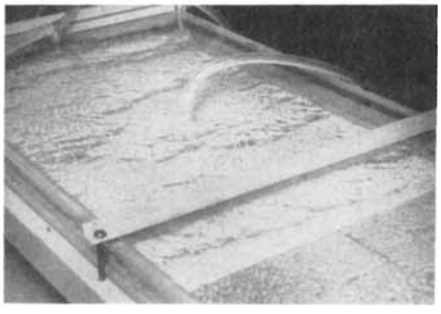

Fig. 7. Photograph of roll waves.

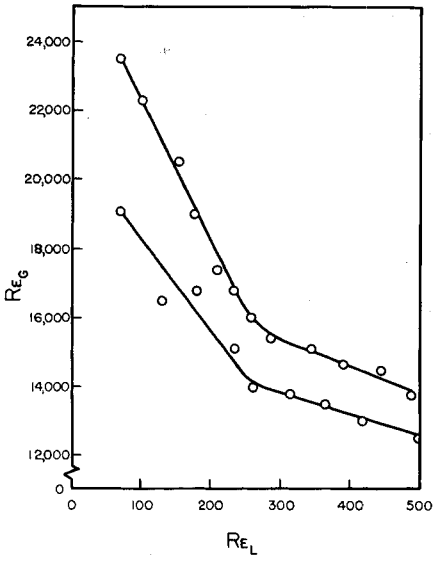

Fig. 8. Re_G vs. Re_L for third transition.

The Re_G range, 1,000 to 5,000, over which two-dimensional waves first formed, was in the same range as the transition to turbulence in the gas phase; however, the appearance of a disturbed liquid surface was not coincident with the transition to gas-phase turbulence. In some runs a smooth surface coexisted with a fully developed gas-phase turbulence. Likewise transition to a disturbed surface was possible without the existence of a fully developed turbulent gas flow.

Squalls

The two-dimensional wave structure existed only over a small portion of the range of variables investigated. If the air velocity is increased slightly above the first transition point, the two-dimensional waves break into a squall surface, which is shown in Figure 6. These are characterized by a "pebbled" appearance having a wave length of 0.5 to 1 cm. and a width nearly equal to the wave length. The breakdown first appeared as a streak "slicing" down through the two-dimensional waves about 4 to 5 ft. from the point of liquid entry. A slight increase in the air velocity then caused a complete breakup into squalls traveling at nearly the same velocity as the two-dimensional waves.

A second transition was defined at the point where the first streaks appeared. In all cases the transition point did not depend on whether it was approached from high or low gas velocities. The appearance of the squall surface depended on the liquid flow properties; this relation is summarized in Table 4. For Re_L greater than 100 the range of maximum gas velocities (U_{max}) at which this second transition occurred was from 10 to 12 ft./sec. Figure 4 shows a plot relating Re_G to Re_L at the transition. Values of Re^* have been calculated and are presented in Table 5. The second transition appears to be characterized by a value of Re^* of about 600.

The height of the liquid film calculated from Equation (4), a laminar flow being assumed, was much lower than the measured height.

Roll Waves

The squall surface was stable over a wide range of gas flows. Eventually, however, as the gas rate was increased roll waves appeared on the squall surface. This might be analogous to the slugging observed in two-phase flow in pipes. A slug of liquid was picked up and carried over the top of the liquid surface by the gas at a very rapid rate. Figure 7 shows these roll waves. They traversed the complete width of the channel for high Re_L but were only 3 to 4 in. long at low Re_L. They traveled about 2 ft./sec. while the squalls still present traveled approximately 1 ft./sec. The squalls formed a few inches from the liquid entry section,

but the roll waves required 3 to 4 ft. to form.

A third transition was defined as the point where the roll waves first appeared and it was found to be coincident with the point where they disappeared when Re_L was greater than 250. When Re_L was less than 250 the point of transition was dependent on whether the roll waves were appearing or disappearing. The transition was easily determined; however the data were not reproducible. Figure 8 reports the range of variables over which this transition occurred. The parameter Re^* could not be evaluated because of the difficulty of accurately measuring the thickness of the liquid film.

Dispersed Flow

At extremely high flow rates droplets are torn from the liquid surface and the liquid becomes dispersed in the gas phase. At $Re_L = 470$ and $Re_G = 39{,}300$ ($U_M =$ 83 ft./sec.), small droplets began to appear on the top wall of the channel; for $Re_L = 387$ the Re_G must equal 45,100 ($U_M = 95$ ft./sec.); at $Re_L = 69$ the Re_G must be 84,500 ($U_M = 178$ ft./sec.). As the liquid film becomes thinner, or as the Re_L becomes smaller, it becomes much more difficult to disperse the liquid phase.

Effect of the Liquid Surface upon the Gas Flow

The interaction of the roughened liquid surfaces upon the gas is reflected in the form of the velocity profiles and in the magnitude of the shear stress at liquid-gas interface.

Velocity profiles measured at the first and second transition points showed no distortion. (See Figure 9.) However, as the gas velocity was increased past the second transition point an increased interfacial shear stress and therefore a distorted velocity profile was obtained. As shown in Figure 10, the shift of the U_{max} from the center line was 0.075 in. The surface was quite rough during this run. It possessed a pebbled appearance, the height of each "pebble" being estimated at about 0.010 in. Run 54, shown in Figure 10, and run 14, shown in Figure 11, have nearly the same Re_L (127 and 170 respectively) and different Re_G; however the velocity profiles are very similar. Figure 12 shows the velocity profile for run 55 with Re_L equal to 508. This shift of U_{max} from the center is nearly 0.140 in. The same is true in run 56, which is shown in Figure 13. At higher values of Re_L thicker films resulted and the squall surfaces became rougher. The height of the "pebbles" in runs 55 and 56 was close to 0.030 in. The interfacial shear stress and therefore the distortion of the velocity profile appear to be related to the height of the roughnesses on the liquid surface.

The velocity-profile data for runs 14, 54, 55, and 56 have been plotted as u^* vs. log y^* in Figure 14. The solid line

Table 2—First Transition

Run No.	Re_G	Re_L	U_{max} (ft./sec.)	Liq. vel. (ft./sec.)	Liq. ht. (in.)
17	3320	146	9.00	0.109	0.18
18	2560	287	7.03	0.203	0.19
19	4140	11.9	11.0	0.0097	0.17
20	2920	147	7.80	0.110	0.18
21	2090	303	6.10	0.222	0.19
22	945	492	3.80	0.323	0.21
23	2490	257	7.04	0.173	0.20
25	2120	347	6.30	0.222	0.21
27	2090	255	6.40	0.164	0.21
29	2860	156	7.96	0.107	0.20
31	3380	102	8.80	0.074	0.19
33	1330	442	4.40	0.276	0.22
35	5510	37.5	15.1	0.0325	0.16
*37	2270	151	6.50	0.102	0.20

*Run taken at U_{max} only 80% of U_{max} for first transition.

Table 3—Values of $Re^* = hU_\tau\rho_l/\mu_l$ for the First Transition

Run No.	Re_G	Re_L	h (in.)	U_τ (ft./sec.)	Re^*
15	3100	490	0.191	0.39	520
16	8600	20	0.076	1	540
17	3300	150	0.181	0.33	420
19	4100	12	0.166	0.45	530

represents data obtained by Laufer (*4*) for smooth-walled channels; the hollow points represent the profiles from the top dry wall and are in approximate agreement with Laufer's data; the solid points represent the profiles from the rough liquid surface. These data are parallel to the dry-wall data but are displaced downward. They appear to be of the form observed for artificially sand-roughened surfaces. "Equivalent sand roughnesses" k_s have been calculated from Equation (11). Table 6 shows the values of k_s, for runs 14 and 54, about

Table 4—Second Transition

Run No.	Re_G	Re_L	U_{max} (ft./sec.)	Liq. vel. (ft./sec.)	Liq. ht. (in.)
24	3970	275	11.0	0.192	0.18
26	3790	347	10.1	0.245	0.19
28	4000	258	10.9	0.178	0.20
30	4170	156	11.3	0.116	0.18
32	4390	104	12.0	0.078	0.17
34	3240	442	9.0	0.283	0.21
36	8100	37.5	19.9	0.048	0.10
39	4020	151	11.1	0.107	0.20

Table 5—Values of $Re^* = hU_\tau\rho_l/\mu_l$ for the Second Transition

Run No.	Re_G	Re_L	h (in.)	U_τ (ft./sec.)	Re^*
24	4000	260	0.181	0.46	580
26	3800	350	0.191	0.44	590
28	4000	260	0.196	0.46	640
30	4200	160	0.181	0.48	610
32	4400	100	0.171	0.50	600
34	3200	440	0.211	0.38	560
36	8100	38	0.106	0.88	660

0.007 in., and for runs 55 and 56, about 0.03 in. These were the approximate sizes of the roughnesses on the pebbled liquid surface.

DISCUSSION OF RESULTS

The results of the experiments described in this paper on a flowing liquid film are in qualitative agreement with observations of the effect of wind velocity upon the surface of large bodies of water (*5*) and of experimental investigations of the effect of blowing air over a container of water (*6*). They should present further insight into the problem of understanding the role of an air stream in initiating wave formation on a liquid surface. The present experimentation shows that the transition from one type of surface to another depends upon the flow conditions of the liquid film. Thin water films or films of low Re_L are more stable. The characterization of the film stability in terms of the parameter $Re = (hU_\tau\rho_{liquid})/\mu_{liquid}$ is suggested from the results. Not enough data were obtained to support the universality of this parameter. The effect of the pebbled liquid surface upon the gas flow appears to be the same as that of a surface artificially roughened with sand of approximately the same size as the wavelets.

The quantitative results presented for the initiation of a surface instability are not adequately described in terms of theories in the literature. An excellent survey of these theories has been presented by Ursell (*5*). Neither the analysis of Kelvin based on frictionless fluid streams nor the "sheltering" theory of Jeffrey give the same dependence of the stability on the liquid flow properties as evidenced from the experiments reported in this paper; however there is an approximate quantitative agreement between the experimental velocity required to raise waves at first and that predicted by these theories.* Recently analyses of the problem based on the Orr-Sommerfeld equation have been presented in the literature (*7, 8*). Yih (*7*), who analyzed the case of a film flowing down a vertical fall, predicted a critical $Re_L = 1.5$. This is very much smaller than the values

*This agreement has been pointed out by C. V. Sternling, who drew up the following comparison:

Formulas:

Jeffrey's analysis	Frictionless case
$U = 4.4(\mu_L g/\rho_G)^{1/3}$	$U = 1.41(g\rho_L g G/\rho_G^2)^{1/4}$
$c = \frac{1}{3}U$	$c = \sqrt{\rho_G/\rho_L}\,U$
$\lambda = 2\pi c^2/g$	$\lambda = \pi c^2/g$

Comparison with data:

	Jeffrey	Frictionless	Experimental
U, cm./sec.	107	608	130 to 460
c, cm./sec.	35.7	23.2	23 to 30
λ, cm.	8.1	1.73	1 to 1.25

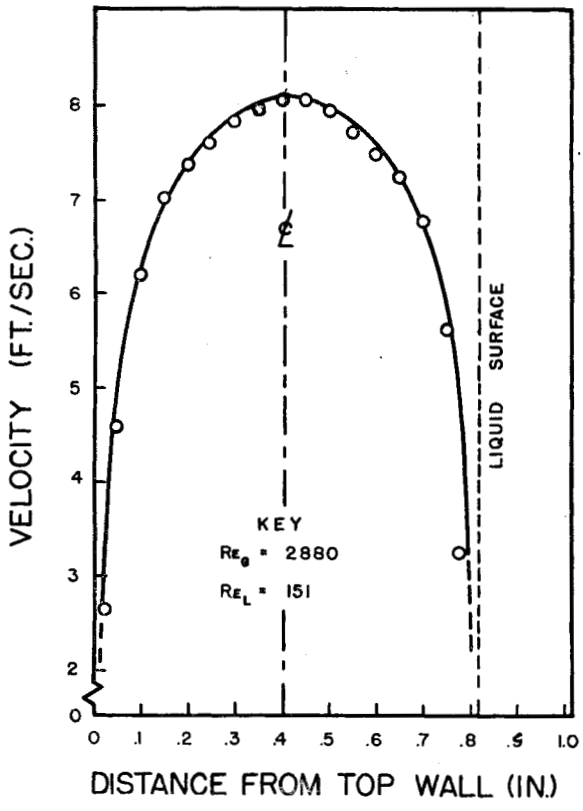

Fig. 9. First-transition velocity profile, run 38.

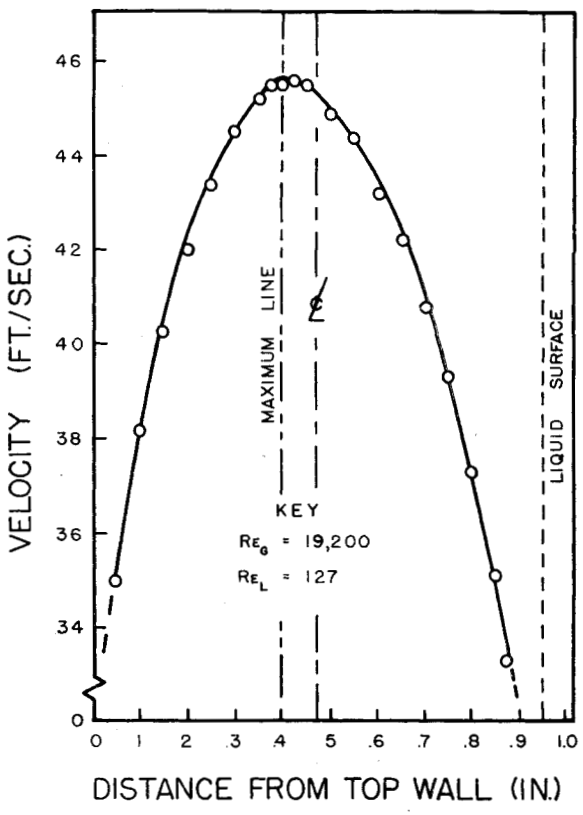

Fig. 10. Third-transition velocity profile, run 54.

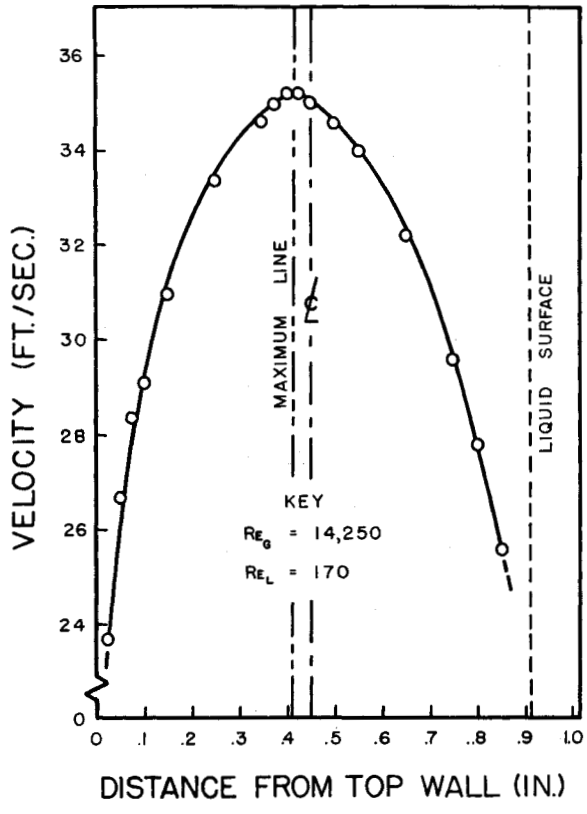

Fig. 11. Velocity profile, run 14.

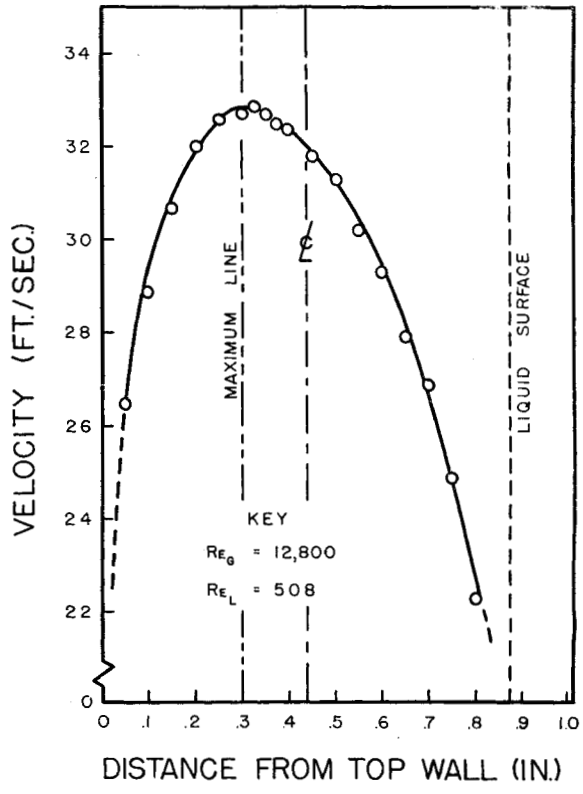

Fig. 12. Velocity profile, run 55.

TABLE 6
EQUIVALENT SAND ROUGHNESSES

Run No.	Re_G	Re_L	U_{max} (ft./sec.)	τ_{0_1} (lbs./ft.²)	τ_{0_2} (lbs./ft.²)	k_s (in.)
14	14,250	170	35.2	0.00661	0.00787	0.0077
54	19,200	127	45.6	0.00852	0.0117	0.0061
55	12,800	508	32.9	0.00562	0.0107	0.036
56	13,900	508	35.6	0.00623	0.0116	0.030

reported here. (See Table 2.) Experimental measurements of Keulegan (*6*) on the initiation of waves in a basin of water on the bottom of a channel through which air was blown gave critical gas velocities in the range of 200 to 900 cm./sec. The experiments reported in this paper involved a flowing liquid film; the basic flow field in the water was quite different from that in Keulegan's experiments. A direct comparison is therefore not possible; however, the critical gas velocity in the two investigations is of the same magnitude.

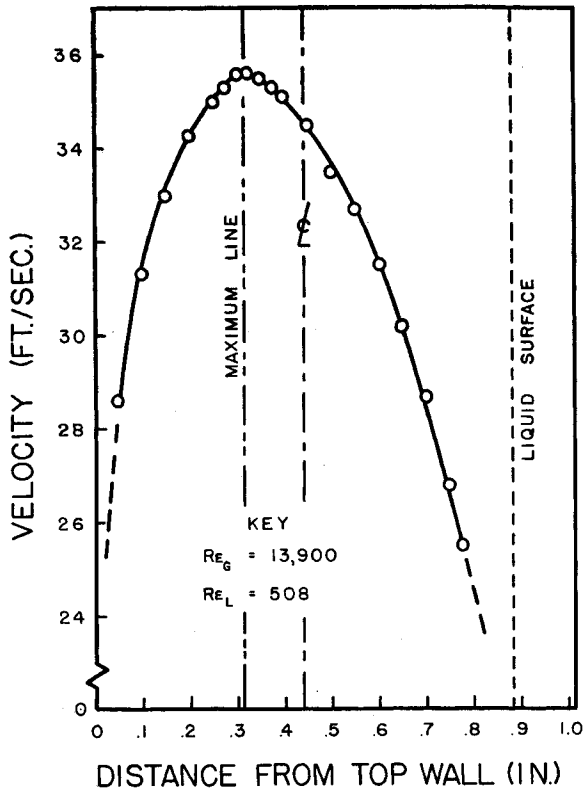

Fig. 13. Velocity profile, run 56.

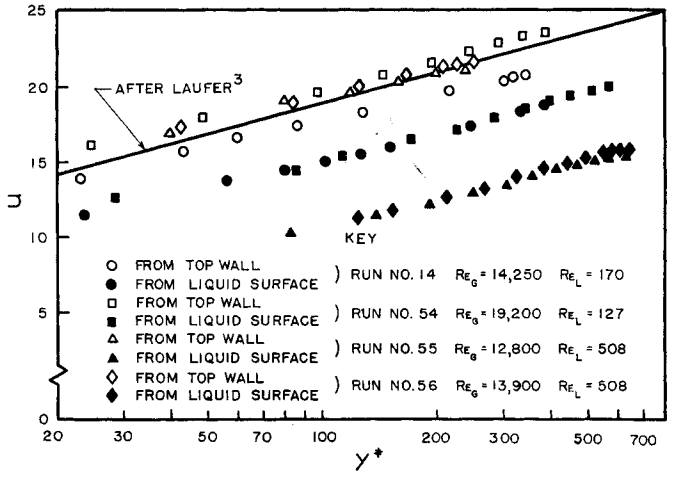

Fig. 14. Comparison of data with Laufer's velocity measurements in dry channel.

ACKNOWLEDGMENT

The idea for this research program came from discussions with C. V. Sternling and R. R. Hughes of Shell Development Company, and the research was partially supported by the Office of Ordnance Research. The authors are grateful for their interest.

NOTATION

- a = distance from maximum in velocity profile to top wall
- b = distance from maximum in velocity profile to liquid surface
- c = wave velocity
- g = gravitational constant
- h = liquid film thickness
- H = thickness of the gas phase
- k_s = equivalent sand roughness
- λ = wave length
- P = pressure
- ρ = density
- Q = volumetric liquid flow rate
- Re_G = gas-phase Reynolds Number $(HU_m\rho/\mu)$
- Re_L = liquid-phase Reynolds number $(hQ\rho/S\mu)$
- Re^* = surface characterization parameter $hU_\tau\rho/\mu$
- S = cross-sectional area of the channel
- t = time of oscillation
- T = surface tension
- τ_{0_1} = shear stress at the top wall
- τ_{0_2} = shear stress at the liquid surface
- u = liquid velocity in x direction
- U = point gas velocity in x direction
- U_m = mean gas velocity $(1/H \int_0^H U\, dy)$
- U_{max} = maximum gas velocity
- u^* = velocity parameter U/U_τ
- U_τ = friction velocity $(g_c\tau_0/\rho)^{1/2}$
- μ = viscosity
- v = liquid velocity in y direction
- w = liquid velocity in z direction
- W = liquid weight rate of flow
- y = distance from a surface
- y^* = distance parameter $yU_\tau\rho/\mu$

LITERATURE CITED

1. Lamb, Horace, "Hydrodynamics," 6 ed., pp. 363-475, Cambridge University Press (1953).
2. Schlichting, Hermann, "Boundary Layer Theory," McGraw Hill Book Company, Inc., New York (1955).
3. Engen, James M., M.S. thesis, Univ. Illinois, Urbana (1956).
4. Laufer, John, *Natl. Advisory Comm. Aeronaut. Rept.* 1053 (1951).
5. Ursell, F., "Surveys in Mechanics," p. 216, Cambridge University Press (1956).
6. Keulegan, Garbis, H., *J. Research, Natl. Bur. Standards*, **46**, no. 5, 358 (1951).
7. Yih, Chia-Chun, "Proceedings of Second U. S. National Congress of Applied Mechanics," p. 623 (1955).
8. Lock, R. C., *Proc. Cambridge Phil. Soc.*, **50**, 105–24 (1954).